Bursting of a high pressure bubble through a free surface

B.Y. Ni *[a,b]
a. College of Shipbuilding Engineering, Harbin Engineering University, Harbin 150001, P. R. China;(nibaoyu@hrbeu.edu.cn)
b. Department of Mechanical Engineering, University College London, London WC1E 7JE, UK;

Highlights:

- The bursting of a fully submerged bubble with high internal pressure has been simulated.
- A methodology has been developed to deal with the sharp corner formed when the bubble surface merges with the free surface after it breaks up.
- Physics of the oscillation of the free surface in the form of a long and thin jet with a much higher second peak after bubble bursting has been discussed.

1. Introduction

Bubble bursting at the free surface can be found in biological, chemical and geophysical fields, as well as in nuclear engineering. It is suggested that it plays an important role in the natural production of liquid nuclei at the sea surface (Wu, 2002, Zhang et al., 2012), in the damages caused by the underwater explosion bubbles (LeMéhauté & Wang, 1995), as well as the cell damage observed in bioreactors as a result of bursting bubbles (Boulton-Stone & Blake, 1993, Boulton-Stone,1995).

In mathematical modelling and numerical simulations, bubble bursting at the free surface always presents a huge challenge due to the complex deformation and rapid motion of the air/liquid interfaces. Especially for a fully submerged bubble with large initial internal pressure relative to the ambient pressure, it will rise to the free surface and burst open very violently. Once it is open, this is often accompanied by a jet shooting up from the bottom of the bubble. When the jet reaches its peak height, it will fall down due to the gravity. The free surface will then oscillate and a second peak or more may appear before its deformation diminishes gradually through wave propagation away to the far field (Kedrinskii, 1978, LeMéhauté & Wang, 1995, Georgescu et al., 2002). Longuet-Higgins (1983) adopted a Dirichlet hyperboloid to model the bursting of an axisymmetric bubble. Since the deformation of the bubble surface could be expressed in an analytical form in this problem, he was able to show when the angle between the asymptotes of the hyperboloid reduces and approaches to $2\arctan\sqrt{2}$, both the velocity and acceleration at the tip of the hyperboloid become infinity. Based on this critical condition, LeMéhauté & Wang (1995) assumed that the bubble would simply break up at the apex at this very moment. In this kind of problem, as soon as the bubble bursts, there arises a major challenge in the numerical scheme. This is because two different directional normals exist at the intersection point of the bubble surface and free surface. This may cause a singularity which would greatly affect the stability of the numerical procedure if it is not properly resolved. LeMéhauté & Wang (1995) assumed that the unknown normal velocity remained single valued at the sharp corner, the same as other collocation points on the free surface and it was obtained by solving boundary integral equation directly. The tangential velocity was taken as the weighted average of those on the two elements attached to the corner. The normal direction at the corner was chosen as that perpendicular to the tangential velocity direction. However, mathematically to assume the normal at the sharp tip of the jet is single valued is not wholly justifiable. When the tip is an important part of the solution, this may cause numerical inaccuracy and instability. Thus a suitable scheme has been developed in this work to deal with the sharp tip after bubble bursting. This allows such a highly complex problem to be modelled successfully. In the present work the whole process of bubble motion and the free surface motion will be simulated, including the bubble rising/bursting, jet development, free surface rising/falling, wave oscillation and propagation.

2. Mathematical Model and Numerical Method

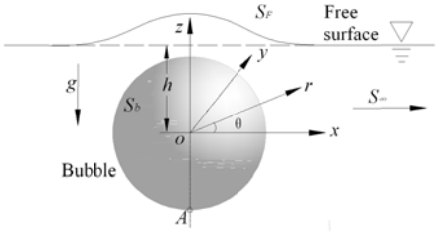

Fig. 1 Sketch of the problem with Cartesian and cylindrical coordinate systems

Fig.1 gives a sketch of the problem, which shows an initial spherical bubble close to a free surface. The distance between the initial bubble centre and the undisturbed free surface is h. When the internal pressure is spatially constant, the mathematical problem is axisymmetric about z. The fluid is assumed inviscid and incompressible, and the flow is irrotational. Thus, a velocity potential Φ can be introduced, which satisfies Laplace's equation

$$\nabla^2\Phi = 0, \tag{1}$$

in the fluid domain.

On the bubble surface and free surface, the fully nonlinear kinematic and dynamic boundary conditions can be written as below in the Lagrangian framework:

$$\frac{Dr}{Dt} = \frac{\partial\Phi}{\partial r}, \qquad \frac{Dz}{Dt} = \frac{\partial\Phi}{\partial z}, \tag{2}$$

$$\frac{D\Phi}{Dt} = \frac{1}{2}|\nabla\Phi|^2 - gz + \frac{P_\infty - P_l}{\rho}, \tag{3}$$

where D/Dt is the substantial derivative following a fluid particle, ρ is the density of the liquid, g is the acceleration due to gravity, P_∞ is the ambient pressure. Because the origin of the coordinate system is set at the

initial bubble centre, one has $P_\infty = P_{atm} + \rho g h$, where P_{atm} is the atmospheric pressure. P_l is the local fluid pressure on the surface, one has $P_l = P_g - \sigma\kappa$ when considering the surface tension, where σ is the surface tension coefficient, κ is the local surface curvature, and $P_g = P_b$ on the bubble surface, or $P_g = P_{atm}$ on the free surface.

It is assumed that the gas inside the bubble satisfies an isentropic law. Thus the pressure P_b inside the bubble is related to the volume V through the following equation (Lamb, 1975):

$$P_b = P_0 (V_0 / V)^\tau , \qquad (4)$$

where P_0 and V_0 are respectively the initial gas pressure and volume when the bubble is generated, τ is the ratio of specific heat of gas. This state equation is applicable up to the moment of bubble breaking up, after which the bubble pressure is just taken as the atmospheric pressure $P_b = P_{atm}$.

Just before the rupture of the bubble, when the water layer between the bubble surface and the free surface becomes very thin, the element sizes used must be comparable to the thickness of the liquid layer. However, the element size cannot be reduced continuously indefinitely, which is one of the main reasons for the difficulty in analysing the micro details of extremely thin water layer. One way forward is to assume the water layer will break up when this is sufficiently thin (Ni et al., 2013). Here it is assumed that when the smallest distance between the nodes on the bubble surface and on the free surface is less than a critical value $\Delta\bar{s}_{c1}$, the bubble will open up at this point at the next time step. Also the bubble surface near this point with its distance to the free surface is smaller than another critical distance $\Delta\bar{s}_{c2} \geq \Delta\bar{s}_{c1}$ will open up. In this way $\Delta\bar{s}_{c1}$ will decide the moment of bubble bursting and $\Delta\bar{s}_{c2}$ will decide the size of the bubble surface being opened up.

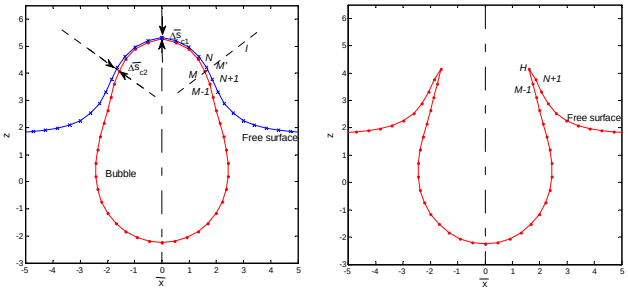

(a) Before bubble breaking (b) After bubble breaking

Fig. 2 Sketch of numerical procedure for a bubble bursting through the free surface

For the axisymmetric case considered here, it is observed during the simulation that the node on the bubble with the shortest distance to the free surface is its top point, as shown in Fig.2. The distance between the nodes on the bubble surface and on the free surface with $\bar{x} = 0$ is firstly defined as $\Delta\bar{s}_1$. When $\Delta\bar{s}_1 \leq \Delta\bar{s}_{c1}$, the water layer is regarded to be sufficiently thin and the bubble will burst in the next time step. To decide the size of the opening, we define a line l through point M on the bubble surface along its normal direction. The line intersects with the free surface at M', which is located in the element with nodes N and N+1. Variables such as velocity potential on M' are obtained by interpolation from nodes N and N+1. When the distance between points M and M' $\Delta\bar{s}_2 < \Delta\bar{s}_{c2}$ the water layer will be just cut there in the next time step, as shown in Fig.2(b). After the bubble is opened up, the point of intersection between the bubble surface and free surface is marked as H, whose location and velocity potential are taken as the average of those at points M and M'.

In the subsequent calculation, care must be taken at the intersection point H, because the normal derivatives Φ_{n1} and Φ_{n2} from the both sides of the sharp corner of H are different. When calculating the corresponding coefficient in the matrix at the intersection, the integral can be split into two parts: one from the integration over the left side surface and the other from the right side surface. However, there exists one more unknown in this case, and one extra condition needs to be found before solving the matrix equation.

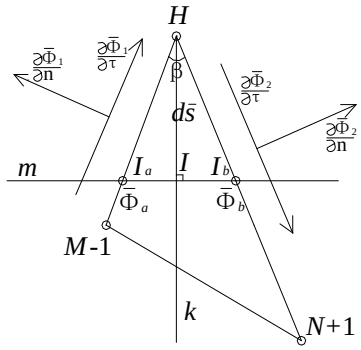

Fig. 3 Numerical treatment on the sharp corner

This is provided from a numerical scheme shown in Fig.3. Assume the angle between the two segments at the sharp corner is β. Bisect the angle β by using a line k. Draw a line m perpendicular to k with the intersection point I, whose distance to point H is $d\bar{s}$ which is quite small, and line m will intersect the two segments at I_a and I_b respectively. Assume the potentials at these points are Φ_a and Φ_b respectively. One can get the derivative $\Phi_{(I_b I_a)} = (\Phi_b - \Phi_a)/s_{ba}$, where s_{ba} is the distance between the points I_a and I_b. The weighted average of projections along the line m of normal derivatives Φ_{n1} and Φ_{n2}, as well as tangential derivatives $\bar{\Phi}_{\tau 1}$ and $\bar{\Phi}_{\tau 2}$ should be equal to $\bar{\Phi}_{(I_b I_a)}$. This gives a link between Φ_{n1} and Φ_{n2}, which can be used an extra condition for the matrix equation. Then the total velocity (Φ_r, Φ_z) at H can be obtained by the weighted average of those on the two sides of the corner, which is used to update the potential and the free surface shape. The calculation is then allowed to continue.

3. Results and discussions

A case is chosen here to show the jet formations after bubble bursting, rapid free surface deformation and wave propagation. Results for the velocity field and pressure contour are provided. Nondimensionalisation is applied based on the initial bubble radius R_0, the ambient pressure P_∞ and the density of the fluid ρ. Thus $Fr = \sqrt{P_\infty / \rho g R_0}$ as the Froude number, $\varsigma = P_0 / P_\infty$ as the strength parameter, $We = R_0 P_\infty / \sigma$ as the Weber number and $\lambda = h / R_0$ as the distance parameter are introduced. The dimensionless parameters in this case are taken as: $\varsigma = 20$, $Fr = 2.5$, $We = 2.2 \times 10^6$, $\lambda = 1.7$ and $\tau = 1.25$ (Cole, 1965).

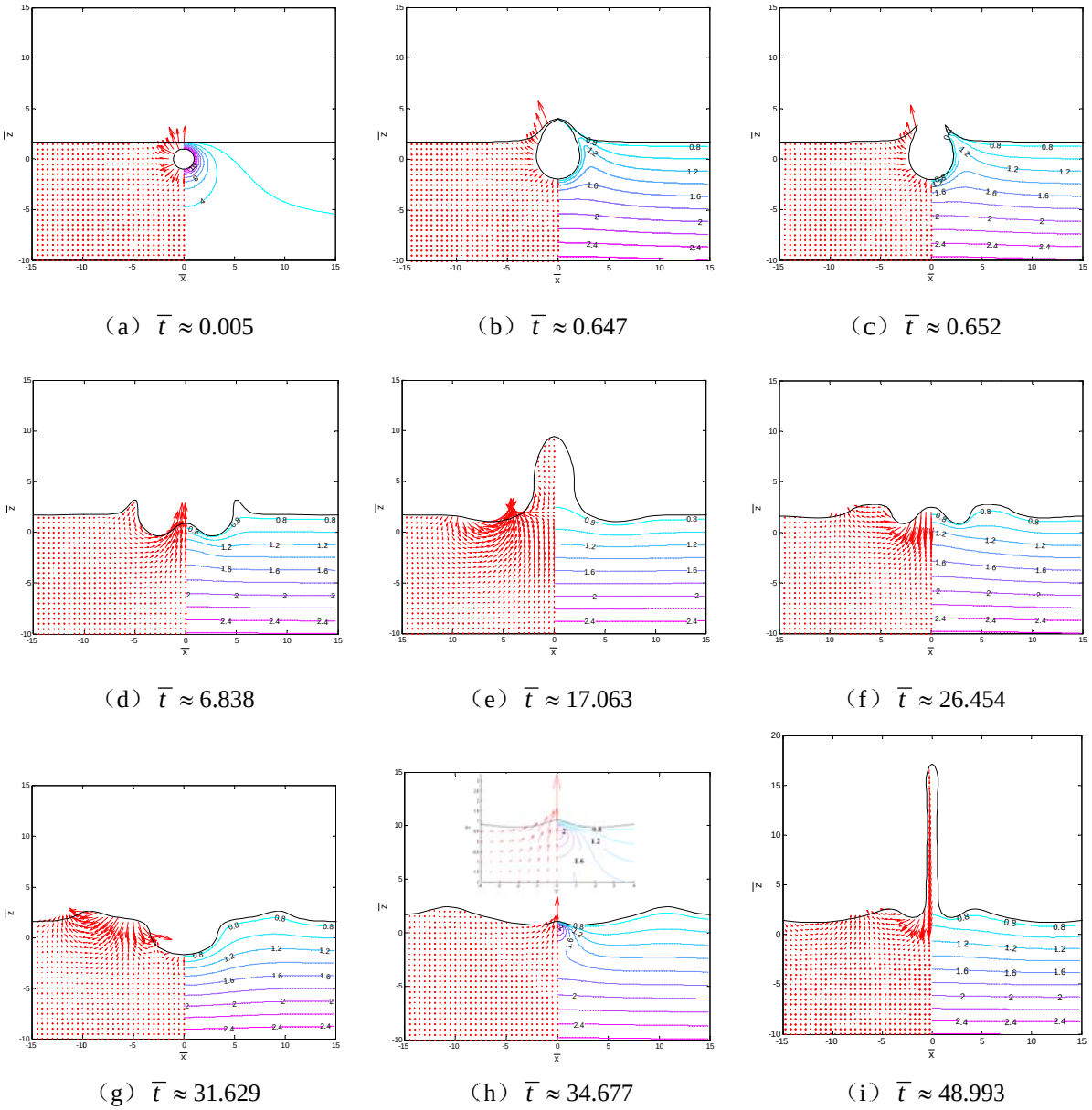

（a） $\overline{t} \approx 0.005$　（b） $\overline{t} \approx 0.647$　（c） $\overline{t} \approx 0.652$

（d） $\overline{t} \approx 6.838$　（e） $\overline{t} \approx 17.063$　（f） $\overline{t} \approx 26.454$

（g） $\overline{t} \approx 31.629$　（h） $\overline{t} \approx 34.677$　（i） $\overline{t} \approx 48.993$

Fig.4 Velocity vectors and pressure contours for $\varsigma = 20$, $Fr = 2.5$, $We = 2.2 \times 10^6$ and $\lambda = 1.7$. Arrow lengths are scaled with respect to the maximum instantaneous velocity in each frame.

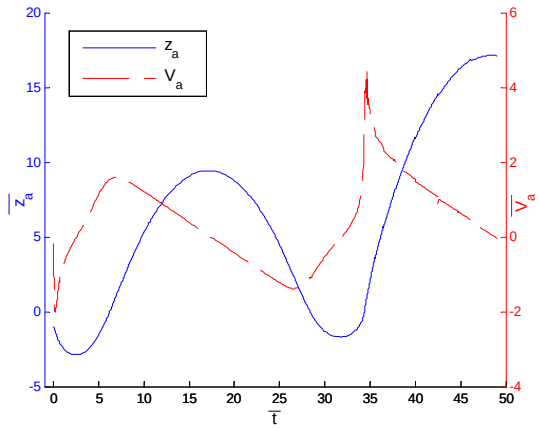

Fig.5 The time-history of the vertical coordinate and velocity of point *A*

Fig. 4 provides the pressure contours and velocity vectors near the bubble and free surface as well as the evolution of the bubble and free surface and Fig.5 gives the variation of the vertical coordinate and the velocity of point *A*, which is the lowest point initially on the bubble surface as shown in Fig.1. Initially the gradient of the pressure at the top of the bubble is higher than that at the bottom of the bubble because of the difference in the hydrostatic pressure. Thus the induced radial velocity at the top of the bubble is larger due to a larger initial acceleration, as shown in Fig.4(a). As the bubble expands, its top moves towards the free surface, while its bottom or point *A* moves downwards as shown in Fig.5. The pressure inside the bubble then reduces gradually. Fig.4(b) presents the surfaces right before bubble bursting and it is found that at this time step $P_b / P_{atm} \approx 1.01$. The water layer is removed in the next time step, and the bubble is opened up as shown in Fig.4(c). After this moment $\overline{t} \approx 0.652$, the pressure at point *A* becomes P_{atm}. This creates a larger local pressure gradient shown in Fig.4(c), which leads to a larger acceleration, as shown in Fig.5. Due to momentum point *A* still goes downwards. It continues until it reaches the first bottom at $\overline{t} \approx 2.584$. Due to the large hydrostatic pressure at lower position, point *A* then moves up with rapidly rising velocity. The velocity reaches a peak and then it slows down and becomes zero at $\overline{t} \approx 17.063$ when point *A* reaches its first peak, as shown in Fig.5. A large hump of the free surface around point *A* is formed, as shown in Fig.4(e), and much of the kinetic energy of fluid is converted into the potential energy. It can also be seen in Fig.4(e) that the hydrodynamic pressure inside the hump is almost P_{atm}. This means that gradient of the pressure is near zero. From the momentum equation, one can infer that the vertical acceleration of the fluid particle is $-g$. This coincides well with what has been observed in Fig.5, in which there is a section with a constant acceleration $-g$ during $6.84 \le \overline{t} \le 26.66$. The elevated free surface is pulled down by the gravity as the time progresses. Point *A* reaches the bottom second time at $\overline{t} \approx 31.629$ as shown in Fig.5. Fig.4(g) gives the surface shape at this moment. The location of point *A* is not as low as that of the previous trough. The deformation of the free surface becomes evident over a larger area, which indicates disturbance or generated wave is propagating outwards. Almost right after point *A* reaches the second trough, the surrounding water starts rushing towards the centre, leading to a higher pressure gradient at point *A*, as shown in the local magnification in Fig.4(h). The acceleration at point *A* becomes extremely large, shown by the nearly vertical velocity curve in Fig.5. It leads to a much larger velocity peak of 4.34 at $\overline{t} \approx 34.677$ before it slows down. Consequently, point *A* reaches a much higher peak. However, this is followed only by those points near point *A* or those slightly away from the centre. As a result a long and thin jet is formed at $\overline{t} \approx 48.993$, as shown in Fig.4(i). Then the jet column will be pulled down by the gravity and point *A* will continue to oscillate but with gradually reduced peaks as the disturbance propagates outwards in the form of the surface wave.

Acknowledgements

This work is supported by Lloyd's Register Foundation through the joint centre involving University College London, Shanghai Jiaotong University and Harbin Engineering University, the National Natural Science Foundation of China (Nos. 11302056 and 11302057), and the International Postdoctoral Exchange Fellowship Program (No. 20140068), to which the authors are most grateful. Lloyd's Register Foundation helps to protect life and property by supporting engineering-related education, public engagement and the application of research.

References:

[1] Boulton-Stone J. M., Blake J. R., Gas bubbles bursting at a free surface, Journal of Fluid Mechanics, 1993, 254: 437–466P

[2] Boulton-Stone J. M., The effect of surfactant on bursting gas bubbles, Journal of Fluid Mechanics,1995, 302: 231–257P

[3] Cole R.H., Underwater explosion, New York: Dover, 1965.

[4] Georgescu S. C., Achard J. L., Canot E., Jet drops ejection in bursting gas bubble processes, European Journal of Mechanics B/Fluids, 2002, 21:265-280P

[5] Kedrinskii V. K., Surface effects from an underwater explosion (Review), translated from Zhurnal Prikladnoi Mekhanikii Tekhnicheskoi Fiziki. 1978, 4: 66-87

[6] Lamb H., Hydrodynamics, sixth edition, Cambridge University Press, 1975

[7] LeMéhauté B., Wang S., Water waves generated by underwater explosion, Advanced series on ocean engineering: v.10, 1995, World Scientific Publishing.

[8] Longuet-Higgins M. S. Bubbles, breaking waves and hyperbolic jets at a free surface, Journal of Fluid Mechanics, 1983, 127: 103–121P

[9] Ni B. Y., Zhang A. M., Wu G. X., Numerical and experimental study of bubble impact on a solid wall, ASME-Journal of Fluid Engineering, 2015, 137(3),031206

[10] Wu J., Jet drops produced by bubbles bursting at the surface of seawater. J. Phys. Oceanogr. 2002, 32, 3286–3290.

[11] Zhang J. Q., Chen J. J., Zhou N. J., Characteristic of jet droplet produced by bubble bursting on the free liquid surface, Chemical Engineering Science, 2012, 68:151-156